

Tungsten divertor sources in WEST related to impurity inventory and local plasma conditions

G.J. van Rooij², Olivier Meyer¹, S. Brezinsek³, C Desgranges¹, D. Douai¹, S. Ertmer³, A. Gallo⁴, C. Gil¹, J. Gunn¹, T. Loarer¹, E. Tsitrone¹, the EUROfusion PFC team* and the WEST Team**

¹IRFM, CEA-Cadarache, F-13108 Saint-Paul-lez-Durance, France

²DIFFER - Dutch Institute for Fundamental Energy Research, De Zaale 20, 5612 AJ Eindhoven, the Netherlands

³Forschungszentrum Jülich GmbH, Institut für Energie- und Klimaforschung-plasmaphysik, D-52425 Jülich, Germany

⁴Aix-Marseille Univ, CNRS, PIIM, UMR 7345, Marseille F-13397, France

*<http://www.euro-fusionscipub.org/PFC>

**See <http://west.cea.fr/WESTteam>

E-mail: g.j.vanrooij@diffier.nl

Abstract

A dedicated series of L-mode deuterium discharges were performed in WEST in which a broad parameter space in terms of divertor plasma temperature (inner divertor at <10 eV, outer divertor up to 50 eV) and impurity flux density was achieved by variation of X point elevation, upstream plasma density and fuelling position and rate. Density steps provided stable reference plasma conditions whilst density scans up to the point of detachment revealed the sputtering threshold behaviour of the dominant sputtering species. Tungsten gross erosion was quantified via the common WI 400.9 nm line and correlated with the residual gas content.

Keywords: tungsten erosion, WEST, optical emission spectroscopy, plasma-surface interaction, nuclear fusion

1. Introduction

The WEST (Tungsten-W Environment in Steady state Tokamak) project aims at testing actively cooled tungsten Plasma Facing Components (PFCs) in the Tore Supra device as to prepare for ITER operation^{1,2}. An important aspect of tokamak operation in a tungsten environment is controlling the tungsten impurity pollution in the main plasma^{3,4}. This starts with quantification of the net source at the divertor surfaces⁵ owing to physical sputtering. Hence, in situ characterization of the divertor W sources is an essential element of future PFC testing in WEST.

The present contribution aims at demonstrating the quantitative capabilities of the newly installed spectroscopy system⁶ in this respect. It is based on a consistency check between the tungsten erosion due to physical sputtering and the local impurity inventory, or more precisely, the impurity flux mix hitting W target plate, as measured spectroscopically in dependence of the local plasma conditions as inferred from electric probe measurements.

A dedicated series of L-mode deuterium discharges (I_p -, B_t -, n_e =core range, T_e =core range) was performed at different fuelling and heating rates to scan the divertor plasma conditions, in particular plasma temperatures, over the threshold of physical sputtering of tungsten for the main

plasma impurities, i.e. oxygen, carbon, and tungsten itself⁵. The spectroscopic determination of tungsten sputtering is correlated with line integrated divertor density from infrared interferometry and plasma temperatures and flux densities from Langmuir probe measurements. The experimental results are analysed in terms of effective sputter yield and absolute sputter rates.

2. Experimental

A dedicated series of Ohmic and Lower Hybrid (LH-) heated discharges in lower single null configuration were executed ($I_p = 500$ kA, $B_t = 3.6$ T, $n_e = 1-4 \times 10^{19}$ m⁻³, $T_e = 2$ keV). Aimed was at a low divertor temperature regime ($T_e < 10$ eV) to cover the threshold for physical sputtering of tungsten by the main plasma impurities, i.e. oxygen and carbon (sputtering of deuterium ions sets in at around 300 eV⁵, which is not reached in L-mode divertor conditions). The comparison with LH-heated discharges allowed a larger temperature variation, equivalent to a spread in the impact energy of the impurity ions, at the inner strike point as well as offered the opportunity to investigate the effect of tungsten sources outside of the divertor. In the Ohmic discharges, fuelling rate was adjusted to achieve integrated divertor densities in the range $1 - 5 \times 10^{18}$ m⁻². The LH-heated discharges included 0.8

– 3 MW additional heating at a roughly constant line integrated density of $1 \times 10^{18} \text{ m}^{-2}$. In both cases, two plateau phases of 2 s were included in a single pulse to ensure stable and steady state conditions (e.g. eliminating dynamics due to plasma cooling from the sputtered W). In addition, density ramps were performed to capture the threshold behaviour of the physical sputtering.

Passive emission spectroscopy was used on the common WI 400.9 nm atomic line to quantify tungsten gross erosion at the solid tungsten monoblocks of the WEST lower divertor. Details of the spectroscopy system can be found elsewhere⁶. The absolute radiance calibration was performed during the shutdown following the experiments, i.e. two months afterwards. Errors from the calibration are expected to be negligible compared to e.g. uncertainties in the local S/XB values (see below). The inner strike point was monitored with 26 lines of sight as sketched in Figure 1 (with a typical distance of 0.85 cm between neighboring lines of sight). The sputtered tungsten flux density (Γ_W in $\text{m}^{-2}\text{s}^{-1}$) was inferred from the absolute line radiation measurements (Φ in $\text{m}^{-2}\text{s}^{-1}$) following the inverse photon efficiency, S/XB, method [Behringer]:

$$\Gamma_W = \frac{S}{XB}(T_e) \times \Phi_W \quad (1)$$

The S/XB value varies significantly in the plasma temperature regime that was under investigation ($T_e < 10 \text{ eV}$)⁷:

$$\frac{S}{XB}(T_e) = 53.7(1 - 1.04e^{-T_e/22.1}) \quad (2)$$

As accurate temperature information was not yet available at the time resolution of the spectroscopy measurements, we interpreted most of the data on basis of the tungsten line emission. The rationale behind this approximation is that otherwise statistical errors in the average temperature might obscure trends in the erosion fluxes. The disadvantage is that the temperature regime under evaluation (5-10 eV) involves a change in S/XB by a factor of 2. In other words, line radiation of neutral W atoms at 5 eV is twice as efficient compared to radiation at 10 eV. Hence, sputtering as reported in the present paper is overestimated by a factor of up to 2 as the divertor temperatures was decreasing towards 5 eV.

Divertor plasma parameters were monitored on basis of Langmuir probe measurements. The electric probes are positioned at locations representative of the conditions viewed by the spectroscopy and allow a spatial resolution of 12 mm. For the density ramps, the low-density low-temperature conditions were too challenging for the probe analysis to provide the required temporal resolution. Instead, infrared interferometry was used to monitor the instantaneous divertor density (LID1 viewing the divertor as indicated in Figure 1)⁸.

Residual gas analysis (RGA) on a midplane pumping duct during the post-discharge recombination phase of the discharge was used to estimate the global oxygen content on basis of partial pressures of O_2 , CO_2 and H_2O . Such a quantitative analysis for carbon was not possible due to a

complex hydrocarbon signature. The carbon content was also estimated from the RGA measurements by considering masses from 12 to 20, correcting for the contribution from water, and assuming $\text{C}_x\text{H}_y\text{D}_z$ molecules. It is noted that errors are inherently large and unpredictable for inferring carbon content from the RGA measurements due to complexity of the hydrocarbon distribution and the large acquisition time of 7s compared to the peaking in the time evolution of the hydrocarbon release.

3. Results

An overview spectrum recorded in WEST around the line of interest, the WI 400.9 transition, is shown in Figure 2. It confirms the presence of the two main impurities oxygen and carbon. The signature of the molecular CD band indicates that carbon is (transiently) present at the surfaces in the strike point areas. Also, a WII line is indicated. Overlap with the OII transition inhibits any analysis of prompt redeposition from the WII/WI line ratio. Such an analysis would require information on WII lines in the UV⁹, a spectral range for which the WEST spectroscopic system has insufficient sensitivity.

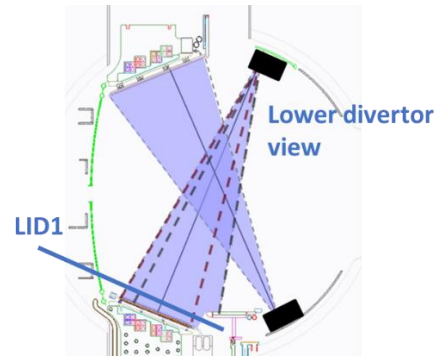


Fig 1: Layout of the spectroscopy system that was used to quantify tungsten sputtering in the WEST lower divertor. Also indicated is the infrared interferometry line of sight monitoring the divertor line integrated density, LID1.

Measured profiles of the tungsten 400.9 line radiation are plotted in Figure 3. The dual effect of increasing the divertor density, i.e. decreasing divertor temperature by increasing the divertor density and hence the target flux, is clearly observed in the Ohmic pulses. Initially, the increased density drives a larger flux whilst the temperature is still in the plateau region of the sputter yield (i.e., the sputter yield is still independent of the divertor temperature). This reasoning is under the assumption of a constant impurity concentration throughout the experiments. Consequently, the tungsten source increases, as observed in the increased tungsten emission. Only after reaching the threshold regime, the temperature effect on lowering the sputter yield starts to dominate and a roll-over in the sputter source is observed.

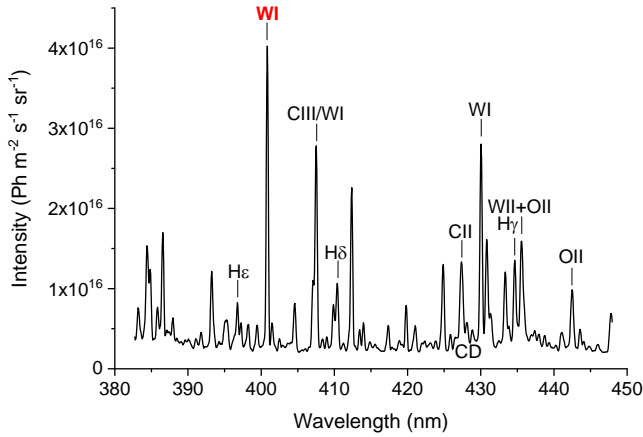


Fig 2: Overview spectrum recorded in WEST showing the well resolved WI 400.9 nm line, Balmer lines, as well as the presence of the main impurities, i.e. oxygen and carbon.

Langmuir probe measurements were difficult to interpret as the low x-point configuration caused unfavourable grazing incident field lines and influenced the apparent ion saturation currents. Inspection of individual measurements at the strike point maximum indicated that electron temperatures ranged between 7 and 9 eV before the roll-over was observed. The roll-over occurred at 5-6 eV. This temperature regime corresponds to the sputtering threshold of O⁴⁺ and C³⁺.¹⁰ We note that the charge state determines the acceleration of the ion over the plasma sheath and thus the response of the effective sputter yield to the plasma temperature. C³⁺ is the dominant charge state at 10 eV, O⁴⁺ is also not unlikely due to transport from upstream higher temperature regions.

The additional LH-heating affects also the magnetic equilibrium and moves the inner strike point further inboard. The shape and particularly the width of the strike point are unaffected. More importantly, the tungsten emission increases roughly proportional with the divertor density. Hence, we conclude (in absence of an independent measurement of the impurity mix) that the impurity mix is not significantly altered by the applied LH heating.

A density ramp was executed to assess the roll-over in the tungsten sputtering in more detail. The inner strike point electron temperature was initially 10 eV, as was inferred from Langmuir probe data. The signal-to-noise in the probe measurements was insufficient to extract temperature data resolving the dynamics of the pulse. Hence, we estimate the electron temperature from the infrared interferometry line integrated density assuming that the power delivered to the surface remains unchanged. Two-point model scaling predicts a scaling of divertor temperature with the divertor density to the power -2/3 (which follows from inserting formula 5.11 into 5.10 of Stangeby¹¹). Although it may not be evident that two-point model scaling is truly applicable to the scrape off

layer for the present experiments, it will not introduce large errors given the small temperature range for which it is used here, i.e. < 5eV.

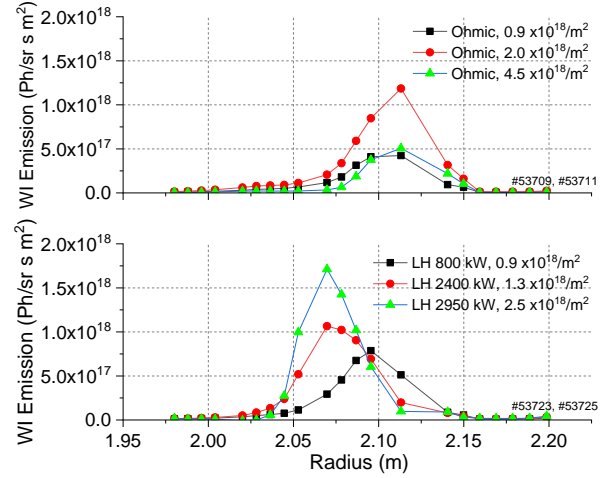


Fig 3: Tungsten emission profiles at the WEST inner strike point in scans of divertor fuelling and LH heating. The profiles are 1 s averages in the plateau phases of the discharges.

The response of the tungsten emission in the density ramp is plotted in Figure 4. Using the two-point model scaling, it indicates that the sputtering roll-over sets in at a divertor temperature of ~8 eV and has decreased by a decade at a temperature of ~6 eV. We note once more that not taking into account any changes in S/XB in the present analysis implies an overestimation of the sputtering by up to a factor of 2 at the lowest temperature of 5 eV. The finite tungsten radiation that is observed at the end of the density ramp is the result of a baseline effect in the automatic line integration procedure and reflects the (systematic) error in the analysis.

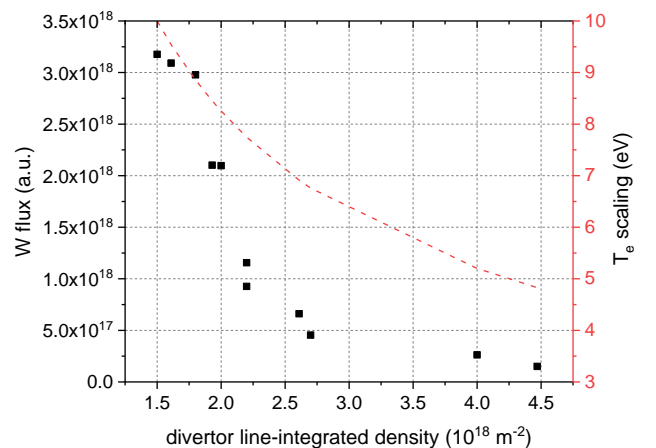


Fig 4: Evolution of the inner strike point tungsten emission in an Ohmic density ramp. The initial divertor temperature was 10 eV, the final temperature is estimated at 5 eV.

The effective sputter yield (i.e. with respect to the incident total particle flux) is estimated on basis of the emission profile in Figure 3 for the Ohmic $0.9 \times 10^{18}/\text{m}^2$ line integrated plasma density discharge phase. Given the divertor temperature of $T_e \cong 10$ eV, we find $S/XB=18.2$ (from eqn 2). Integrating over the full solid angle and assuming torroidal symmetry (which is not valid given the significant field ripple in WEST)) gives a tungsten sputter rate of $1 \times 10^{20} \text{ s}^{-1}\text{m}^{-2}$, hence an effective sputter yield of 1.6×10^{-3} . This value is similar to the yields that were observed in ASDEX Upgrade¹². It is tenfold higher than in the first ITER-like wall campaign at JET¹³, largely due to the lower sputtering rate of the lighter Be ions that were the main impurity.

The actual effective sputtering value implies an oxygen and/or carbon concentration of ~3%. Here, we assume that both impurities have equal sputtering rates, which is reasonable given the uncertainty in charge state distribution. Residual gas analysis indicates an oxygen and carbon content of roughly 1% and 0.5%, respectively, for these discharges. Firstly, these numbers give an idea of the (relative) importance of both impurities for generating the tungsten source in WEST. Secondly, it demonstrates a good agreement (given the uncertainty in the residual gas analysis estimates) between observed W source and global impurity level. Furthermore, whilst evidently the total impurity level is similar to the early observations in ASDEX Upgrade¹², the lower level of carbon in the present set of WEST discharges is counterbalanced by a higher oxygen concentration.

4. Discussion and conclusions

The tungsten divertor source has been quantified at the inner strike point in the WEST lower divertor. The accuracy of the presented results was mainly determined by limitations in the Langmuir probe measurements. Given the low temperature regime in which the S/XB factor is strongly temperature dependent, this causes the S/XB factor to be ill-defined. The estimated uncertainty in divertor temperature of 5 eV gives at 10 eV an uncertainty in S/XB and thus sputter flux of about 50%.

The absolute sputter rates were $1-2 \times 10^{20} \text{ s}^{-1}$ for the present pulse series. Oxygen and carbon are consistent as main sputtering species, contributing roughly equally, whereas no strong evidence has been found that self sputtering by tungsten is significant. The effective sputter yield was estimated at 1.6×10^{-3} (dropping to essentially zero after reaching ~5 eV), a value similarly to observations in ASDEX Upgrade¹² (with carbon as main sputtering species) and tenfold higher than in the first ITER-like wall campaign at JET¹³ (where lighter Be ions caused the sputtering). These results are promising for controlling the W source in view of the observed relatively modest (intrinsic) carbon concentrations and assuming that oxygen levels can be further improved by wall conditioning.

Acknowledgements

This work has been carried out within the framework of the EUROfusion Consortium. The views and opinions expressed herein do not necessarily reflect those of the European Commission.

References

1. Bourdelle, C. *et al.* WEST Physics Basis. *Nucl. Fusion* **55**, (2015).
2. Bucalossi, J. *et al.* The WEST project: Testing ITER divertor high heat flux component technology in a steady state tokamak environment. *Fusion Eng. Des.* **89**, 907–912 (2014).
3. Joffrin, E. *et al.* First scenario development with the JET new ITER-like wall. *Nucl. Fusion* **54**, (2014).
4. Fedorczak, N. *et al.* Tungsten transport and sources control in {JET} {ITER}-like wall {H}-mode plasmas. *J. Nucl. Mater.* **463**, 85–90 (2015).
5. Den Harder, N. *et al.* ELM-resolved divertor erosion in the JET ITER-Like Wall. *Nucl. Fusion* **56**, (2016).
6. Meyer, O. *et al.* Development of visible spectroscopy diagnostics for W sources assessment in WEST. *Rev. Sci. Instrum.* **87**, 1–4 (2016).
7. Brezinsek, S. *et al.* Spectroscopic determination of inverse photon efficiencies of W atoms in the scrape-off layer of TEXTOR. *Phys. Scr.* **T170**, 14052
8. Gil, C. *et al.* Renewal of the interfero-polarimeter diagnostic for WEST. *Fusion Eng. Des.* **140**, 81–91 (2019).
9. Van Rooij, G. J. *et al.* Tungsten divertor erosion in all metal devices: Lessons from the ITER like wall of JET. *J. Nucl. Mater.* **438**, (2013).
10. Naujoks D, Asmussen K, Bessenrodt-Weberpals M, Deschka S, Dux R, Engelhardt W, Field AR, Fussmann G, Fuchs JC, Garcia-Rosales C, Hirsch S, Ignacz P, Lieder G, Mast KF, Neu R, Radtke R, Roth J, Wenzel U, A. upgrade team *et al.* Tungsten as target material in fusion devices. *Nucl. Fusion* **36**, 671 (1996).
11. Stangeby, P. C. *The Plasma Boundary of Magnetic Fusion Devices.* (2000).
12. Dux, R. *et al.* Plasma-wall interaction and plasma behaviour in the non-boronised all tungsten ASDEX Upgrade. *J. Nucl. Mater.* **390–391**, 858–863 (2009).
13. van Rooij, G. J. *et al.* Tungsten divertor erosion in all metal devices: Lessons from the {ITER} like wall of {JET}. *J. Nucl. Mater.* **438, Suppl**, S42–S47 (2013).